JOURNAL OF MATERIALS SCIENCE 33 (1998) 1927–1931

Characterization of albumin- and lysozyme–adsorption evaluated on two differently prepared apatites

TOSHIYUKI AKAZAWA
Hokkaido Industrial Research Institute, Nishi-11, Kita-19, Kita-ku, Sapporo, Hokkaido 060-0819 Japan

MASAYOSHI KOBAYASHI, TOHRU KANNO
Department of Chemical System Engineering, Kitami Institute of Technology, 165 Koencho, Kitami, Hokkaido 090 Japan

KOHEI KODAIRA
Division of Materials Science and Engineering, Graduate School of Engineering, Hokkaido University, Nishi-8, Kita-13, Kita-ku, Sapporo, Hokkaido 060 Japan

Ca^{2+}-deficient hydroxyapatite (r-HAp) originated from cattle bones and stoichiometric hydroxyapatite (s-HAp) derived from reagents were prepared by wet syntheses. The adsorption characteristics of albumin (BSA) and lysozyme (LSZ) on the two HAp surfaces were compared by changing the heating temperature of the powders at 273–1073 K in a stream of water vapour. The saturated amount of adsorption (A_{SA}(B) for BSA and A_{SA}(L) for LSZ) on these HAp powders changed little at 273–673 K (Region I), but at 673–1073 K (Region II), clearly increased with crystallite size growth and transformation of crystal morphology. As far as the surface proportions of HAp for P- and C-adsorption sites (the ratios $A_{SA}(L)/A_{SA}(B)$) are concerned, r-HAp gave no change in Region I and decreased in Region II, whereas those for s-HAp were kept constant through all regions. The heats of LSZ adsorption, Q_L, for r-HAp and s-HAp, respectively, increased and decreased in Region II. These differences could be a result of the Ca^{2+}-deficient structure of r-HAp with the OH^--vacancy and loosening surface structure due to segregation of impurities in Region II. r-HAp exhibited a 157% higher heat of BSA adsorption, Q_B, and a 60% lower Q_L in Region I than s-HAp. Conclusively, r-HAp can be used as an excellent adsorbent, rather than s-HAp, because of its chromatographic characteristics for the separation of acidic and basic proteins. © *1998 Chapman & Hall*

1. Introduction

As is well known, hydroxyapatite [HAp, i.e. $Ca_{10}(PO_4)_6(OH)_2$] has excellent bioaffinity or biocompatibility and characteristics for the adsorption of proteins. The adsorption characteristics of HAp will be governed by the physicochemical nature of the solid surface, which is influenced by crystallite size, pore structure and morphology of particles [1, 2].

The adsorption sites on the surface of hexagonal HAp are classified into two groups [3] : first, a positively charged site (C-site) composed of two Ca^{2+} (screw Ca II) ions located on a rectangle, 0.942 nm in length on the *a*-axis and 0.344 nm in length on the *c*-axis. The other is a negatively charged site (P-site), which is co-ordinated with six O^{2-} ions belonging to three PO_4^{3-} ions and forms a hexagonal double-triangular array. The C- and P-sites on HAp correspond to the vacant positions of an hydroxyl group on the *a*-face and the Ca^{2+} (columnar Ca I) site on the *c*-face, respectively. Provided that the HAp crystals formed are suspended in an aqueous solution with proteins, it is deduced that the OH^- and Ca I^{2+} ions on the HAp surface dissolve minutely and the remaining sites constitute the active C- and P-sites that are available for adsorption of acidic or basic proteins [3].

Bovine serum albumin (BSA) with a terminal group of $-COO^-$ (which is an acidic one-chain protein [4]) and lysozyme from egg white (LSZ) with a terminal group of $-NH_2^+$ (which is a basic one-chain protein [5]) are adsorbed on the C- and P-sites of HAp, respectively [3].

In previous papers [6, 7], it was demonstrated that r-HAp prepared from cattle bones had a larger saturated amount of adsorption and a higher heat of adsorption for BSA than s-HAp prepared from reagents.

As r-HAp is a Ca^{2+}-deficient HAp containing small amounts of metal ions [7], it can be expected that the

fine surface structure and the surface proportion of the C- and P-sites are greatly influenced by the heat treatment conditions. Accordingly the surface characteristics derived thus should contribute to the selective adsorption of BSA and LSZ on each of the active sites.

The first aim of this study is to elucidate heat treatment effects on crystallite size and microstructure of r-HAp and s-HAp. Evaluating the adsorbate ability of the HAp powders prepared, BSA and LSZ were chosen as the representative acidic and basic proteins, respectively. The second aim is to investigate the controlling parameters for the chromatographic separation characteristics of BSA and LSZ when the HAp powders are used as a packing material for liquid chromatography.

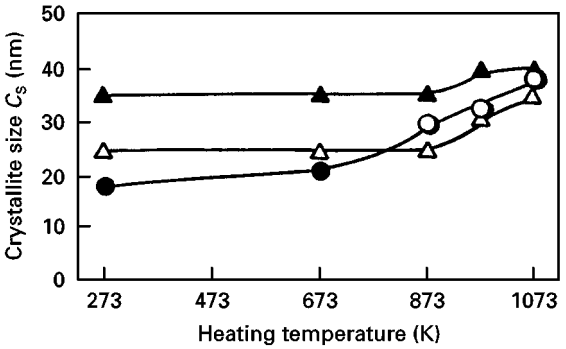

Figure 1 Crystallite sizes calculated from each crystal plane using the Scherrer equation for the HAp powders (○) (2 0 0) of r-HAp, (●) (0 0 2) of r-HAp, (△) (2 0 0) of s-HAp, (▲) (0 0 2) of s-HAp.

2. Experimental procedure

r-HAp was prepared by the following procedure: calcination of cattle bones, dissolution to a 0.2 mol dm^{-3} HNO_3 solution and reprecipitation at 298 K and pH 10.5 [7, 8]. s-HAp was prepared, as a contrasting sample, using guaranteed grade $Ca(NO_3)_2 \cdot 4H_2O$ and $(NH_4)_2HPO_4$ reagents by the wet method [7]. The two HAp powders were heated at 273–1473 K for 24 h in a stream of water vapour balanced with a N_2 gas flow.

The crystalline phases of the powders obtained thus were identified by powder X-ray diffraction (XRD). The crystallite sizes were calculated by Scherrer's equation using the (0 0 2) or (2 0 0) plane of HAp [8]. Field emission–scanning electron microscopic (FE–SEM) photographs of the samples were taken to observe the morphology and microstructural crystallites formed. The compositional ratio of Ca^{2+} to PO_4^{3-} ion (Ca/P) was determined by electron probe microanalysis (EPMA) and chemical analysis methods, such as the chelate titration method [9] and the Mo acid calorimetric method [10]. HAp powders (0.1 g) were added to solutions (10 cm^3) containing 0.3–3.0 mg cm^{-3} BSA or LSZ, which were adjusted at pH 6.9–7.1 using a mixed solution of 20 mmol dm^{-3} KH_2PO_4 and K_2HPO_4. The mixtures were agitated at 282 and 295 K for 80–100 h. After centrifuging the mixtures, the absorbance of the solutions at 280 nm for BSA or LSZ [6, 7] was measured by ultraviolet spectroscopy. The amounts of BSA or LSZ adsorption on the HAp powders were calculated from the absorbance. The heat of adsorption for each protein was determined from the two adsorption isotherms at 282 and 295 K using the Clausius–Clapeyron equation [11].

3. Results and discussion

3.1. Surface modification of HAp derived after heating

The XRD patterns of the two HAps showed that single phase r-HAp was obtained by heat treatment at 273–1073 K for 24 h in a stream of water vapour, and that stoichiometric s-HAp with the composition ratio of Ca/P = 1.67 was formed and its apatite structure was maintained at a wide temperature range of 273–1473 K. At temperatures > 1073 K, r-HAp decomposed partially to β-$Ca_3(PO_4)_2$ and CaO phases because it was a Ca^{2+}-deficient HAp that consisted of Ca/P = 1.65 and contained small amounts of Mg^{2+}, Si^{4+}, Na^+, Ba^{2+} and Sr^{2+} ions as impurities [7].

Evaluating the surface characteristics of the heat-treated HAps, the crystallite size, C_S, was calculated from the XRD patterns using the Scherrer equation and the results are shown in Fig. 1 as a function of heating temperature. According to anisotropic growth of an hexagonal crystal, C_S is separately expressed as C_{Sa} for the (2 0 0) plane and C_{Sc} for the (0 0 2) plane of the HAp structure. The results clearly show two temperature regions in C_S for r-HAp, that little change at 273–673 K (Region I) and gradually grow at 673–1073 K (Region II). For s-HAp, on the other hand, C_{Sa} increases from about 20 to 40 nm at 873–1073 K, but C_{Sc} falls in the narrow range of 35–40 nm through the entire temperature range.

The FE–SEM photographs in Fig. 2 show the microstructure of the two HAp powders heated at 673 and 1073 K for 24 h. One can recognize a clear difference in the morphology of the two HAps. r-HAp transformed significantly from crystallites about 20 nm in length in Region I to sphere-like aggregates 50–100 nm in width showing a sintering effect in Region II. This transformation may be caused by the crystal habit of Ca^{2+}-deficient apatite structure with vacant Ca I and OH^- sites that interfere with growth along the *c*-axis. Hence, stoichiometric apatite (s-HAp) can grow along the *c*-axis giving needle-like particles with 5–10 aspect ratios in Region I and form prismatic crystals with aspect ratios of 3–5 in Region II. This difference in the microstructure of the two HAps should affect the adsorption behaviour of the proteins. Based on these results, one may presume that r-HAp yields a less anisotropic crystal than s-HAp in Regions I and II, as will be discussed further in the following sections.

3.2. Surface proportions of HAp active sites for BSA and LSZ adsorption

The adsorption of BSA or LSZ on all HAp powders obeyed the Langmuir isothermal equation in the

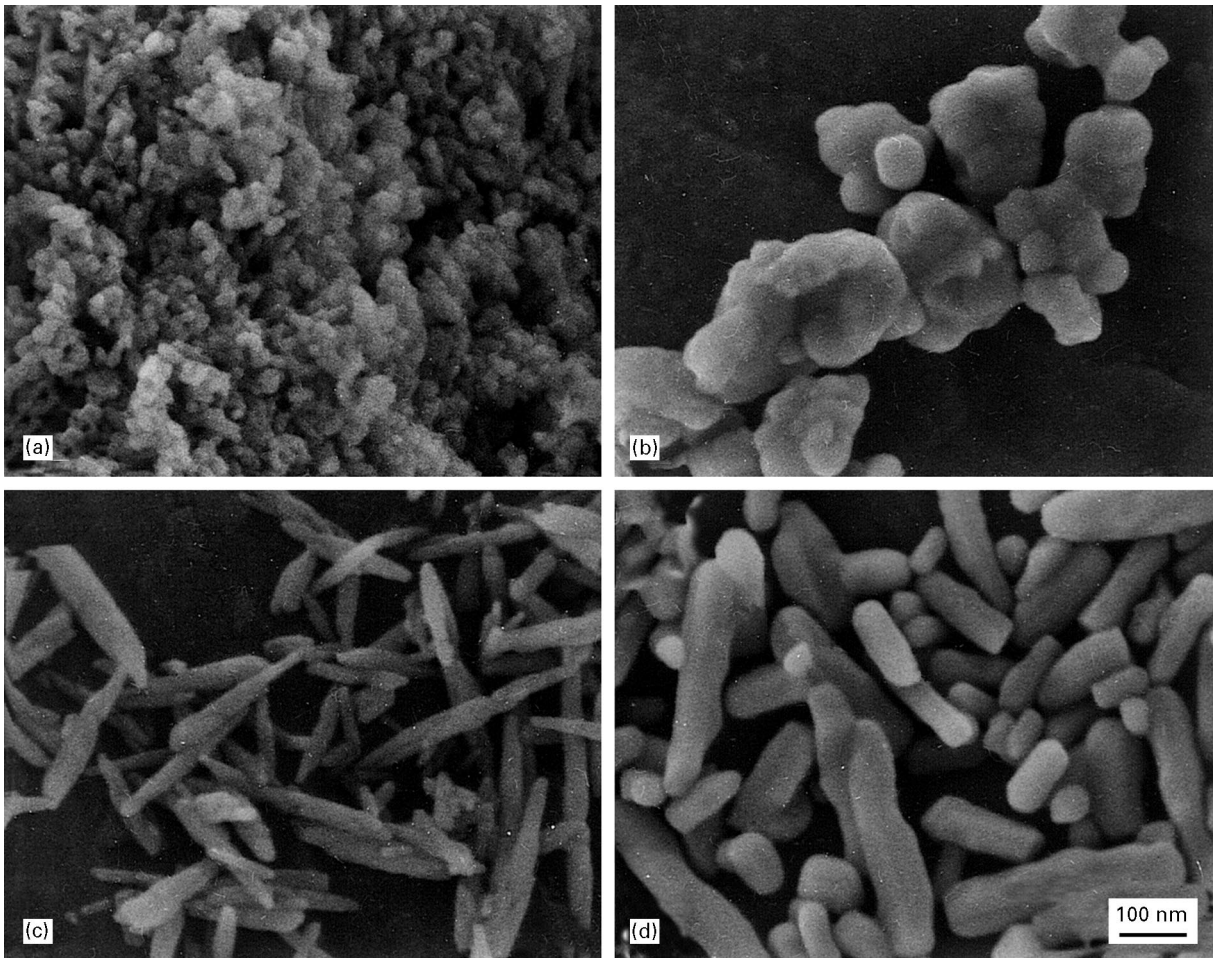

Figure 2 FE–SEM photographs of the HAp powders heat-treated for 24 h in a stream of water vapour: (a) r-HAp (673), (b) r-HAp (1073), (c) s-HAp (673), and (d) s-HAp (1073).

phosphate buffer solutions. Using the equation, the saturated amount of adsorption (designated as $A_{SA}(B)$ for BSA and $A_{SA}(L)$ for LSZ) per surface area of HAp can be calculated and the results are shown in Fig. 3 as a function of heating temperature. $A_{SA}(L)$ for the two HAp powders became three–six times larger than $A_{SA}(B)$ depending on the temperature, indicating that the number of P-sites for LSZ adsorption on the surface of the HAp surface is greater than those of C-sites for BSA adsorption. This phenomenon may be explained by two factors.

1. the high probability of occurrence of the *c*-face on crystal growth, judging from the high C_{Sc} in all the samples; and

2. the crystal habit originating from lattice parameters ($a = 0.942$ nm and $c = 0.688$ nm) of HAp [12].

Moreover, one can recognize again two temperature regions, I (273–673 K) and II (673–1073 K), for the values of $A_{SA}(B)$ and $A_{SA}(L)$. In Region I, no appreciable change is shown. However, in Region II, $A_{SA}(B)$ for the two HAp powders gradually increase and the $A_{SA}(B)$ of r-HAp is 22–44% larger than that of s-HAp, whereas $A_{SA}(L)$ increased from 6.7 to 10.2×10^{-2} μmol m^{-2} for r-HAp and from 6.6 to 12.7×10^{-2} μmol m^{-2} for s-HAp. Based on these results, it can be suggested that the HAp in Region II give different C- and P-site compositions that are respectively available for BSA and LSZ adsorption,

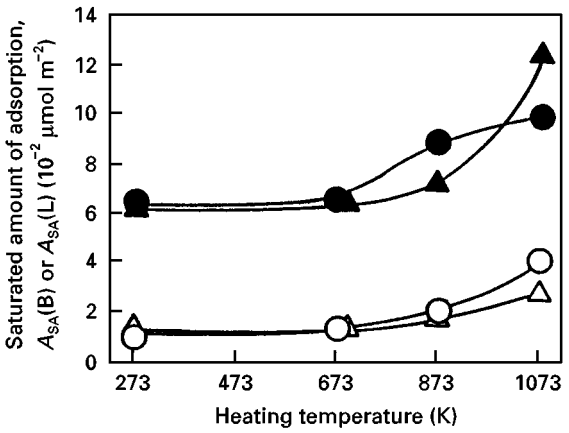

Figure 3 Saturated amounts of adsorption for the two proteins as a function of heating temperature of the HAp powders: (○) BSA on r-HAp, (●) LSZ on r-HAp, (△) BSA on s-HAp, (▲) LSZ on s-HAp.

because they exhibit the different C_S-growth and morphological variation (see Figs 1 and 2).

Fig. 4 shows the ratios of $A_{SA}(L)$ to $A_{SA}(B)$ calculated (designated by R_{SA}) indicating the proportion of P-sites available for LSZ and C-sites for BSA on the HAp surface as a function of heating temperature. The R_{SA} of r-HAp was reduced from 4.88 to 2.41 in Region II, whereas those of s-HAp gave 4.34 ± 0.01 through Regions I and II. To explain the different behaviour of

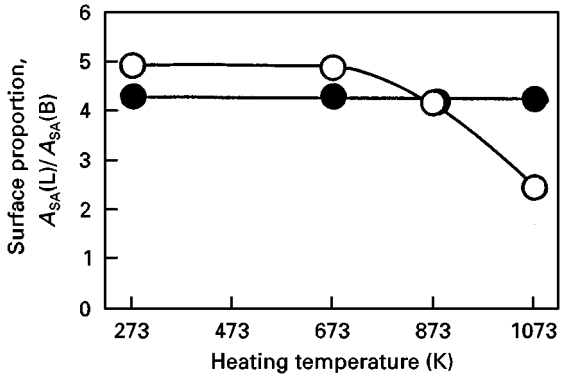

Figure 4 Surface proportions of the saturated amounts of adsorption for LSZ and BSA as a function of heating temperature of the HAp powders: (○) r-HAp, (●) s-HAp.

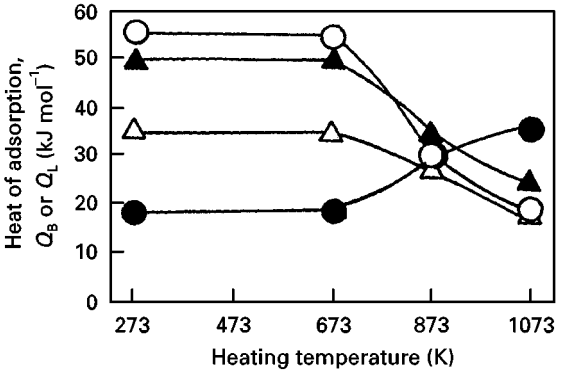

Figure 5 Heats of BSA or LSZ adsorption for the HAp samples as a function of heating temperature: (○) Q_B for r-HAp, (●) Q_L for r-HAp, (△) Q_B for s-HAp, (▲) Q_L for s-HAp.

R_{SA} for r-HAp and s-HAp, two possibilities can be considered:

1. a molecular size difference between BSA and LSZ, which contributes to a difference in the saturated amount of adsorbed molecules derived from the different pore size distributions of the HAp powders, and
2. an active site proportional difference on the HAp powders for the adsorption of BSA and LSZ.

For Case 1, the R_{SA} values in all the HAp powders are not a reflection of the molecular size difference of the two proteins, because the molecular size ratios of LSZ ($3 \times 3 \times 4.5$ nm) to BSA ($4 \times 4 \times 14$ nm) are less than 3.1 in any side-on or end-on adsorption form. Case 1 can thus be rejected. The reduction in R_{SA} is followed by a decrease in the proportion of P- and C-sites, which can be related to an increase in the OH^--vacancy and a loosening effect on the surface structure due to segregation of the metal ions. Case 2 is therefore acceptable.

3.3. Discrimination of surface active sites evaluated by the heats of BSA and LSZ adsorption

To characterize the surface active sites of HAp crystals, the heat of adsorption for BSA, (Q_B), and LSZ, (Q_L), can conveniently be used. Fig. 5 shows Q_B and Q_L, which were calculated by the Clausius–Clapeyron equation as a function of heating temperature for the two HAp powders. The two temperature regions, I and II, are still available for variation of Q_B and Q_L. In Region *I*, Q_B and Q_L for *r*-HAp gave constant values of about 55 and 19 kJ mol^{-1}, respectively; but in Region II, these values varied from 55 to 20 kJ mol^{-1} and from 19 to 36 kJ mol^{-1}, respectively. For s-HAp, on the other hand, Q_B and Q_L in Region I were consistently about 35 and 50 kJ mol^{-1}, whereas the two values in Region II decreased from 35 to 20 kJ mol^{-1} and from 50 to 20 kJ mol^{-1}, respectively. Q_B and Q_L for r-HAp in Region I was 157% higher and 60% lower than the respective values for s-HAp. In Region II, Q_B for r-HAp was very close to the equivalent value for s-HAp. The reduction of Q_B in Region II for the two HAp powders is reasonably explained by C_{Sa}-growth [7]. The adsorption orientation of BSA molecules gradually transform a mixed form of side-on and end-on, to an end-on-rich form on HAp powders. However, the changes in Q_L cannot be interpreted by transformation of the adsorption form.

Based on these results, one can recognize that r-HAp and s-HAp adsorb BSA molecules in similar adsorption form, but have a different LSZ adsorption behaviour which may result from reconstruction of the r-HAp surface structure due to increasing heating temperature.

To clarify the effects of the crystallite morphology of HAp on the adsorption behaviour of BSA and LSZ, Q_B and Q_L are represented in Fig. 6 as a function of C_S. With regard to BSA adsorption on HAp, $A_{SA}(B)$ and Q_B, respectively, increased and decreased with C_{Sc}-growth, regardless of Regions I and II. For LSZ adsorption, Q_L for r-HAp increased anomalously but Q_L of s-HAp decreased with C_{Sc}-growth, although $A_{SA}(L)$ of the HAp samples increased. A possible explanation for the characteristic reverse tendency between Q_B and Q_L may be that the acid strength of the P-sites and the basic strength of the C-sites changed on the HAp surface, as well as the variation in the total number and surface proportion of the C- and P-sites. Especially, on the surface structure of r-HAp with 30–40 nm in C_S, the acid strength on the P-sites for LSZ would be stronger than the basic strength on the C-sites for BSA. This high acid strength can be attributed to the Ca^{2+}-deficient HAp structure because of the ion impurities originating from cattle bones. As the crystallites of r-HAp grow isotropically with heat treatment, they can grow on the *c*-face and give different acid strength of the P-sites compared with s-HAp. Moreover, the P-sites on r-HAp are partially substituted by impurities such as Mg^{2+} and Na^+. If the r-HAp powders heated at higher temperatures are suspended in the LSZ aqueous solution, the impurities segregated on the HAp surface will dissolve minutely because of the loosening structure, so that the remaining sites constitute the active P-sites having high acid strength for LSZ adsorption.

Taking into account these results one may conclude that the two HAp samples originated exhibit different adsorption characteristics of BSA and LSZ and that

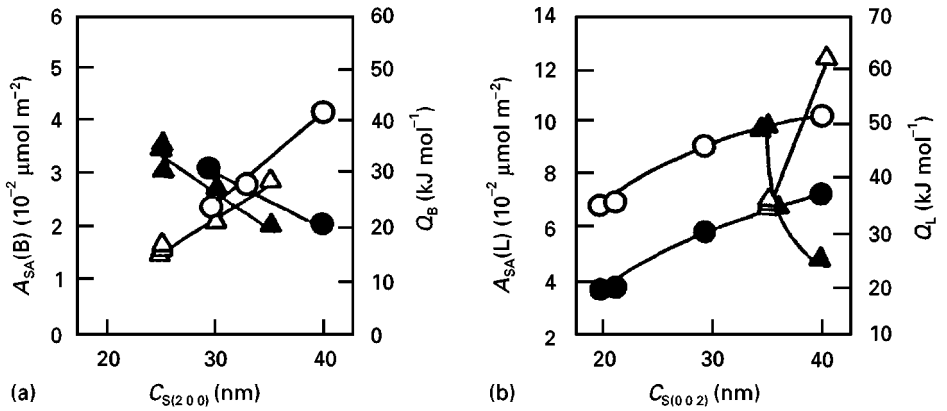

Figure 6 Saturated amounts and heats of (a) BSA and (b) LSZ adsorption for the HAp powders as a function of crystallite size: (○) A_{SA} for r-HAp, (●) Q for r-HAp, (△) A_{SA} for s-HAp, (▲) Q for s-HAp.

the adsorption on r-HAp is strongly influenced by the basic strength of the C-sites or the acid strength of the P-sites, and by the proportions of the two sites, which are reflected by the crystallite size and morphology of HAp depending on the heating temperature. Conclusively, the heating temperature of HAp can be used as a controlling parameter to design a separation column of liquid chromatography for acidic and basic proteins.

4. Conclusions

Ca^{2+}-deficient r-HAp originated from cattle bones and stoichiometric s-HAp derived from reagents by wet methods have different surface structures, such as crystallite size and morphology, depending on the heating temperature experienced, 273–673 K (Region I) and 673–1073 K (Region II). The microstructure in Region I comprised 20 nm length crystallites for r-HAp and needle-like particles with an aspect ratio of 5–10 for s-HAp. In Region II, r-HAp transformed to sphere-like aggregates, 50–100 nm in width; s-HAp formed prismatic particles with aspect ratios of 3–5 and showed a gradual growth in crystallite size.

The saturated amount of adsorption and the heat of adsorption for BSA or LSZ on these HAp powders sensitively varied with C_S growth and the transformation of crystallite morphology, because the acid strength of the P-sites for LSZ and the basic strength of the C-sites for BSA drastically changed on the HAp surface, as well as the total number and surface proportion of the two sites. r-HAp exhibited higher basic strength and lower acid strength than s-HAp in Region I, whereas the strength relation between the two HAp samples was reversed in Region II. These differences in acid or basic strength can be attributed to Ca^{2+}-deficiency of the HAp structure and the metal ions impurities originating from cattle bones. In designing high separation efficiency of liquid chromatography for acidic and basic proteins, r-HAp can effectively be used as an adsorbent by selecting the heating temperature.

Acknowledgements

The authors would like to thank Mr T. Kanazawa, Application and Research Center, JEOL Ltd Co. for his collaboration in the observation of the microstructures using the field emission–scanning electron microscope.

References

1. T. KAWASAKI, K. IKEDA, S. TAKAHASHI and Y. KUBOKI, *Europ. J. Biochem.* **155** (1986) 249.
2. T. KAWASAKI, W. KOBAYASHI, K. IKEDA, S. TAKAHASHI and H. MONMA, *ibid.* **157** (1986) 291.
3. T. KAWASAKI, M. NIIKURA and Y. KOBAYASHI, *J. Chromatogr.* **515** (1990) 91.
4. K. AOKI, T. TAKAGI and H. TERADA, "Kesseiarubumin seitai niokeru sono yakuwari" (Kodansha, Tokyo, 1984) p. 1, p.13.
5. K. IMABORI and H. YAMAKAWA, "Seikagakujiten" (Tokyokagakudojin, Tokyo, 1989) p. 1333–1334.
6. T. AKAZAWA and M. KOBAYASHI, in "Abstracts of the Eleventh Symposium on Inorganic Phosphorus Chemistry", edited by A. Okuwaki (Japanese Association of Inorganic Phosphorus Chemistry, Tokyo, 1996) p. 33–34.
7. *Idem., J. Mater. Sci. Lett.* 15 (1996) 1319.
8. K. ITATANI, O. TAKAHASHI, A. KISHIOKA and M. KINOSHITA, *Gypsum & Lime* **213** (1988) 77.
9. K. UENO, "Kireto Tekiteiho" (Nankodo, Tokyo, 1979) p. 270.
10. Japanese Industrial Standard R9011 (1981) p. 14.
11. T. KEII, "Kyuchaku kyoritsuzensho 157" (Kyoritsushuppan, Tokyo, 1980) pp. 22–9, p. 95–7.
12. Powder Diffraction File No. 9-432, International Centre for Diffraction Data.

Received 4 June 1996
and accepted 5 December 1997